Inorganic Chemistry

Article

pubs.acs.org/IC

Inhibitory Effect of Selenoprotein P on Cu^{+}/Cu^{2+}-Induced $A\beta_{42}$ Aggregation and Toxicity

Xiubo Du,[†,§] Zhi Wang,[‡,§] Youbiao Zheng,[†] Haiping Li,[‡] Jiazuan Ni,[‡] and Qiong Liu*[,†]

[†]Department of Marine Biology, Shenzhen Key Laboratory of Marine Biotechnology and Ecology, Shenzhen University, Shenzhen 518060, China

[‡]College of Life Sciences, Shenzhen Key Laboratory of Microbial Genetic Engineering, Shenzhen University, Shenzhen 518060, China

Supporting Information

ABSTRACT: It has been suggested that the aggregation and cytotoxicity of amyloid-β (Aβ) peptide with transition-metal ions in neuronal cells is involved in the progression of Alzheimer's disease (AD). Selenoproteins are a group of special proteins that contain the 21st amino acid selenocysteine in their sequence, and they are found to be involved in the onset and progression of AD. Here, we report that the histidine-rich domain of selenoprotein P (SelP-H) is capable of binding Cu ions in both oxidation states of Cu^{+} and Cu^{2+} with high affinity and of modulating Cu^{+} and Cu^{2+}-mediated Aβ aggregation, reactive oxygen species (ROS) production, and neurotoxicity. SelP-H was found to coordinate 1 and 2 mol equiv of Cu^{+} and Cu^{2+} with sub-picomolar and nanomolar affinities, respectively. Cu^{+}/Cu^{2+} binding to $A\beta_{42}$ inhibited the fibrillization of $A\beta_{42}$ but induced it to form amorphous aggregates, which could be significantly restored by SelP-H, as observed by thioflavin T fluorescence and transmission electron microscopy. Interestingly, SelP-H inhibited Cu^{+}/Cu^{2+}-$A\beta_{42}$-induced neurotoxicity and the intracellular ROS production in living cells. These studies suggest that SelP may play certain roles in regulating redox balance as well as metal homeostasis.

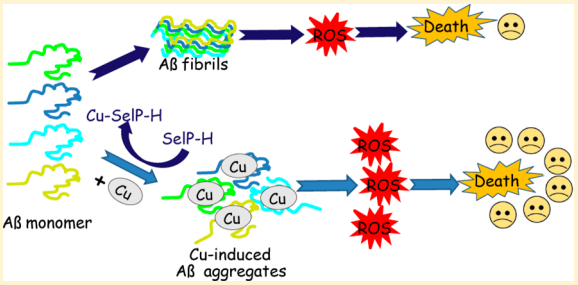

Alzheimer's disease (AD), the leading cause of dementia in elderly people, is now the most common neurodegenerative disease, affecting more than 35 million people worldwide.[1] AD is characterized by two pathological protein deposits, the senile plaques composed mainly of amyloid-β (Aβ) peptide and the neurofibrillary tangles that are bundles of paired helical filaments (PHF) of protein tau.[2] Aβ peptides, the main forms of which are 42 and 40 amino acids long ($A\beta_{42}$ and $A\beta_{40}$, respectively),[3] are generated via cleavage of the amyloid precursor protein (APP) by β- and γ- secretases. $A\beta_{40}$ is present in larger amounts in the brain, yet $A\beta_{42}$ is more neurotoxic and has a higher tendency to aggregate.[4] Dyshomeostasis and miscompartmentalization of metal ions such as Cu, Zn, and Fe ions clearly occur in AD brain. It is suggested that highly concentrated Cu^{2+} plays critical roles in the formation of Aβ aggregates, which are neurotoxic due to the ability of Cu^{2+} to undergo redox reactions at the cell membrane to generate reactive oxygen species (ROS).[5] Of note, Aβ plaques deposited in the AD brain are found to be enriched with metals, particularly with copper.[6] The effects of Cu^{2+} on Aβ aggregation and toxicity were extensively explored; however, little is known of the role of Cu^{+}. Shearer and Szalai found that Aβ binds Cu^{+} with its histidine-13 (His13) and His14 in a linear geometry.[7] The Cu^{+}-Aβ complex may be a critical reactant involved in ROS associated with AD etiology. Traditional metal chelating agents such as clioquinol have been shown to regulate metal-mediated Aβ aggregation and toxicity; however, long-term use of clioquinol is limited by an adverse side effect, subacute myelo-opticneuropathy.[8] A more promising strategy is the use of endogenous metal-binding proteins within the brain to regulate the homeostasis of metal and the subsequent metal-mediated aggregation and toxicity of Aβ. For example, Tan et. al. reported the protective effect of metallothionein-3 against Cu^{2+}-$A\beta_{42}$ aggregates.[9]

Selenoproteins are a group of special proteins that contain the 21st amino acid selenocysteine (Sec) in their sequence. Selenoprotein P (SelP) is the only protein containing multiple (10) Sec residues in the human selenoprotein family and is found in high levels in the brain. It has been suggested that the function of SelP is to encompass oxidant defense and Se homeostasis.[10] The expression of SelP is upregulated in an age-dependent manner[11] and is necessary for the expression of other selenoenzymes, such as GPx4.[10a] Moreover, SelP was found to be colocalized with Aβ plaques in the post-mortem tissue from individuals with the hallmark lesions of AD.[12] The direct association of SelP expression with the pathology of AD suggests that this protein is involved in the response or progression of the disorder. Knockdown of SelP rendered mouse Neuro-2A (N2A) neuroblastoma cells more sensitive to

Received: November 12, 2013
Published: January 17, 2014

dx.doi.org/10.1021/ic4028282 | Inorg. Chem. 2014, 53, 1672−1678

the toxicity of Aβ.[13] However, the exact function and mechanism of SelP in AD prevention remains unknown. The high content of Sec makes SelP a good metalloprotein, since Sec would dramatically outcompete His and cysteine (Cys) for metals, including Cu^{2+} and Cu^{+}. In addition to the high Sec content, SelP is also a Cys- and His-rich protein. It encodes two His-rich regions, located at residues 204−217 and residues 244−250, which were predicted on the surface of the protein by the PROFace program. Recently, we reported that the His-rich domain of SelP (named SelP-H) blocked Zn^{2+}-mediated Aβ aggregation, ROS production, and neurotoxicity.[14] In the present work, the Cu^{+} and Cu^{2+} binding properties of SelP-H were characterized, and its ability to modulate Cu^{+}/Cu^{2+}-mediated $A\beta_{42}$ aggregation and neurotoxicity were discussed.

MATERIALS AND METHODS

Sample Preparation. SelP-H was overexpressed and purified as described previously.[14] SelP-H was treated with 10 mM EDTA for 3 h and then subjected to three rounds of dialysis against appropriate buffer (phosphate-buffered saline (PBS) or *N*-(2-acetamido)-2-aminoethanesulfonic acid (ACES)). Stock solutions of $A\beta_{42}$ (purchased from Chinapeptides Co., Ltd.) were prepared as followed: $A\beta_{42}$ peptide was dissolved in hexafluoroisopropanol (HFIP) to a concentration of 0.5 mg/mL. The solution was incubated at room temperature overnight with shaking and then sonicated in water bath for 15−20 min and dried with N_2 gas. The peptide was finally dissolved in dimethyl sulfoxide (DMSO) thoroughly, sonicated in water bath for another 15−20 min, and used for experiments.

For transmission electron microscopy (TEM) imaging and thioflavin T (ThT) fluorescence, the $A\beta_{42}$ stock solution was diluted in PBS containg 30 μM $CuSO_4$ (with or without 3 mM ascorbic acid (H_2Asc)); then an appropriate amount of apo-SelP-H in PBS was added to the solution, and the mixture was incubated at 37 °C for 24 h before imaging or fuorescence spectra recording. The final concentrations of $A\beta_{42}$, Cu^{2+}/ Cu^{+}, SelP-H are 10 μM. For CCK-8 and ROS assay, the $A\beta_{42}$ stock solution was diluted to a final concentration of 20 μM in fetal bovine serum (FBS)-free Dulbecco's modified Eagle's Medium (DMEM) containing 20 μM $CuSO_4$ (with or without 2 mM H_2Asc), and incubated at 37 °C for 1 h; then an appropriate amount of apo-SelP-H in DMEM was added to the solution, and the mixture was incubated at 37 °C for 24 h before it was added to the cells.

Determination of Cu^{+}-SelP-H Dissociation Constant. Bicinchoninic acid (BCA) is a colorimetric Cu^{+} chelator, which can form a stable purple complex with Cu^{+} in a 2:1 ratio as $Cu^{+}(BCA)_2$ that exhibits absorption maxima at 562 nm (ε = 7900 M^{-1} cm^{-1}) and 358 nm (ε = 42 900 M^{-1} cm^{-1}).[15] Therefore, the transfer of Cu^{+} from BCA to the protein can be monitored by the decrease in UV−vis absorbance of $Cu^{+}(BCA)_2$ at 562 or 358 nm.

Experiments of competitive reactions between BCA and SelP-H or $A\beta_{42}$ were carried out under anaerobic conditions as described previously.[16] Briefly, Cu^{+} in the form of $[Cu(MeCN)_4]PF_6$ was mixed with BCA in a molar ratio of 1:3 in tris(hydroxymethyl)aminomethane (Tris)/HCl buffer (50 mM, pH 7.4) as a stock solution. Protein solutions at various concentrations were then mixed with the stock solution to give rise to a final concentration of Cu^{+} of 20 μM and BCA of 60 μM. Ascorbic acid concentration was kept at 1 mM to maintain the oxidation state of Cu^{+} in the reaction mixture. To ensure the equilibrium was reached, the mixture was incubated at room temperature for at least 1 h (no additional change in absorption was observed). The results were corrected for dilution and baseline absorbance at 800 nm.

Isothermal Titration Calorimetry (ITC). ITC measurements were carried out at 25 °C on a MicroCal iTC-200 microcalorimeter (Northampton, MA). SelP-H was prepared in 20 mM ACES buffer at pH 7.4, with the ionic strength adjusted to 100 mM with NaCl. The titrant was made by mixing appropriate amounts of stock solution of $CuSO_4$ (10 mM in nanopure Milli-Q water) with ACES buffer. The metal concentration of the stock solution was determined by inductively coupled plasma mass spectrometry (ICP-MS).

Briefly, 2 μL of 2 mM $CuSO_4$ were titrated into 200 μL of 50 μM protein over 4 s with a 3 min interval between each injection. Twenty injections were made in total. The reaction solution was stirred at 1000 rpm. The heat of dilution, mechanical effects, and nonspecific interactions were accounted for by averaging the last three points of titration, and the value was subtracted from all data points. The results were analyzed by Origin 7.0 (Microcal) using one-site binding model. A nonlinear least-squares method was used to obtain the best fit parameters for the number of binding sites *n*, the association constant *K*a, and the change of enthalpy ΔH (Supporting Information, Table S2). All of the experiments were performed in triplicate under the same conditions.

Transmission Electron Microscopy (TEM). $A\beta_{42}$ (10 μM) incubated in the presence or absence of Cu^{2+} /Cu^{+} (10 μM) and SelP-H (10 μM) at 37 °C for 6 h. Then each sample (5 μL) was put on glow-discharge Formvar/carbon 300 mesh copper grids and incubated at room temperature for 2 min. Excess solution was removed with filter paper, and the grids were rinsed twice with H_2O. Then the grids were stained with uranyl acetate (1% w/v, H_2O, 5 μL) for 1 min, blotted with filter paper, and dried for 15 min at room temperature. Samples were visualized with a transmission electron microscope (FEI Tecnai G2 TEM) at 200 kV and ×29 000 magnification.

Thioflavin T Fluorescence. The fibrils contents of $A\beta_{42}$ prepared in different conditions were measured by ThT fluorescence. $A\beta_{42}$ (10 μM) incubated in the presence or absence of Cu^{2+} /Cu^{+} (10 μM) and SelP-H (10 μM) at 37 °C for 6 h. The fluorescence spectra of each sample were recorded using a fluorescence spectrophotometer (Fluoroskan Ascent FL 4500, Thermo Scientific) with 444 nm as the excitation filter.

Cell Culture. N2A cells were maintained in DMEM supplemented with 10% FBS, 100 U/ml penicillin G, and 100 μg/mL streptomycin and were cultured at 37 °C, 5% CO_2 incubator. Cells in the logarithmic phase were dissociated with trypsin and seeded in 96-well or 6-well plates, resulting in about 0.5 × 10^3 cells in 100 μL medium or 10^5 cells in 2 mL medium per well, for CCK-8 assay or ROS measurements, respectively. Cells were incubated at 37 °C, 5% CO_2 for 24 h to attach the plates. The $A\beta_{42}$ stock solution was diluted to a final concentration of 10 μM in FBS-free DMEM containing 1 mol equiv of Cu^{2+}/Cu^{+} and incubated at 37 °C for 1 h; then an appropriate amount of SelP-H (with a final concentration of 10 μM) in DMEM was added to the solution, and the mixture was incubated at 37 °C for 24 h before it was added to the cells. For CCK-8 or ROS assay, 50 μL or 2 mL of each preincubated $A\beta_{42}$ sample (with or without the addition of Cu^{2+} /Cu^{+} and SelP-H) was diluted with fresh FBS-free DMEM medium and added individually to the cell well. The same volume of serum-free medium was added into control cultures (only N2A cells present). The cells were then incubated for an additional 24 h at 37 °C. At the end of incubation, the cell viability was determined by CCK-8 assay, and the ROS level was determined by DCF staining.

Cell Viability Assay. Twenty microliters of CCK-8 reagent (Beyotime, Shanghai CHN) was added to each well, and the cells were incubated at 37 °C for another 2 h. The absorbance at 450 nm was measured with a reference wavelength at 650 nm using a SpecTRA MAX 190 mciroplate reader (Molecular Devices, Sunnyvale, CA, USA). Triplicates were performed throughout the procedures.

Measurement of ROS. Before measurement, the old medium was removed from the cells and 2 mL of 2′,7′-dichlorofluorescin diacetate (DCFH-DA, 10 μM in FBS-free medium) were added into each well. Cells were incubated at 37 °C for another 20 min and washed three times with FBS-free medium. Cells were harvested and washed three times with ice-cold PBS and resuspended in PBS. The intensity of fluorescence was analyzed by flow cytometry (FACS Calibur, Becton Dickinson) with excitation at 488 nm and emission at 535 nm. A gate was set to exclude signals from debris and aggregates. Results are expressed as fold change compared with corresponding controls. Ten thousand cells were analyzed in each assay, and assays were run in duplicate.

dx.doi.org/10.1021/ic4028282 | Inorg. Chem. 2014, 53, 1672−1678

RESULTS AND DISCUSSION

SelP-H Binds Cu^+ with High Affinity. As a soft metal, Cu^+ prefers to bind soft ligands (Cys-S or Met-S) with trigonal or tetrahedral geometries. Reports describing His-Cu^+ interactions are emerging; for example, Cu^+ was reported to be ligated by the His13 and His14 in a linear coordination environment in Aβ.[7] The Cu^+ binding affinities and stoichiometry values of SelP-H and Aβ_{42} were determined by competition with BCA. Complexation of Cu^+ to BCA gives rise to $Cu^+(BCA)_2$ with a maximum absorption at 562 nm, Figure 1A, which was used to monitor the competition between the protein and BCA in binding with Cu^+. Addition of SelP-H led to decreases in the absorption of $Cu^+(BCA)_2$ (Figure 1A), indicating the translocation of Cu^+ from BCA to SelP-H. The absorbance data obtained in SelP-H titrated into $Cu^+(BCA)_2$ (Figure 1) were used to calculate the binding constants for the Cu^+-SelP-H complex (Supporting Information, Table S1), using the following equations, where P represents free protein and $n$$Cu^+$-P represents Cu^+-bound protein.

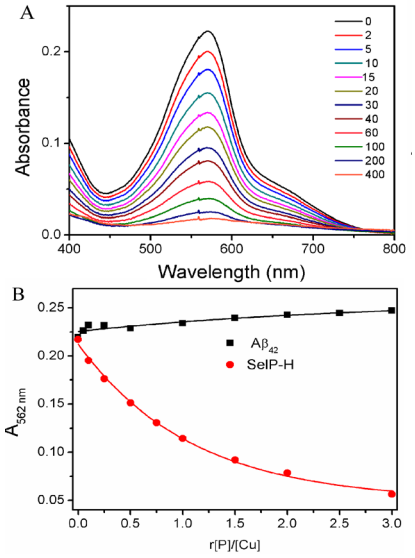

Figure 1. Comparison of the Cu^+ binding affinity between SelP-H and Aβ_{42}. (A) Absorption spectra of Cu^+, ascorbate and BCA, with the addition of 0–20 mol equiv of SelP-H. (B) Absorbance at 562 nm with the titration of SelP-H or Aβ_{42} into 20 μM Cu^+, 60 μM BCA, and 1 mM ascorbate.

$$Cu^+(BCA)_2 + [(n-1)Cu^+\text{-P}] = (nCu^+\text{-P}) + 2BCA$$

$$K_{an} = \frac{[nCu^+\text{-P}][BCA]^2}{[Cu^+(BCA)_2][(n-1)Cu^+\text{-P}]} \quad \text{(Eq.1)}$$

$$Cu^+ + 2BCA^{2-} = Cu(BCA)_2^{3-}$$

$$\beta_2 = \frac{[Cu^+(BCA)_2]}{[Cu^+][BCA]^2} \quad \text{(Eq.2)}$$

The overall formation constant log β_2 for $Cu(BCA)_2$ has been estimated to be 17.3 previously.[17]

Here we assumed that the n binding sites for Cu^+ on SelP-H are independent and equivalent. We take n = 2 first and then generalize the result to cases for which n > 2. The relationships between the equilibrium constants K_{a1} and K_{a2} and the stability constants for Cu^+-SelP-H (K_1), 2Cu^+-SelP-H (K_2) and $Cu(BCA)_2$ (β_2) are given by the following equations.

$$Cu^+ + P = Cu^+\text{-P}$$

$$K_1 = \frac{[Cu^+\text{-P}]}{[Cu^+][P]} = \beta_2 K_{a1} \quad \text{(Eq.3)}$$

$$Cu^+ + (Cu^+\text{-P}) = 2Cu^+\text{-P}$$

$$K_2 = \frac{[2Cu^+\text{-P}]}{[Cu^+][Cu^+\text{-P}]} = \beta_2 K_{a2} \quad \text{(Eq.4)}$$

The fractional saturation Y = (concentration of Cu^+ bound to P)/(total concentration of all forms of P) is given by

$$Y = \frac{[Cu^+\text{-P}] + 2[2Cu^+\text{-P}]}{[P] + [Cu^+\text{-P}] + [2Cu^+\text{-P}]} \quad \text{(Eq.5)}$$

Rearranging Eq.1 and Eq.5 results in Eq.6:

$$Y = \frac{2K_a}{X + K_a} \quad \text{(Eq.6)}$$

where $X = [BCA]^2/[Cu^+(BCA)_2]$, K_a is the intrinsic binding constant, $K_{a1} = 2K_a$, and $K_{a2} = K_a/2$ from a statistical point of view. Therefore

$$\frac{1}{Y} = \frac{1}{2} + \frac{1}{2K_a}X \quad \text{(Eq.7)}$$

Equation Eq.7 is the result obtained for two equivalent sites. In general, for n equivalent sites, it can be written as

$$\frac{1}{Y} = \frac{1}{n} + \frac{1}{nK_a}X \quad \text{(Eq.8)}$$

The slope of the plot of $1/Y$ versus X (Figure 2) gives log K_a = 1.36 × 10^{-4} (correlation coefficient r = 0.99, n = 1.03,

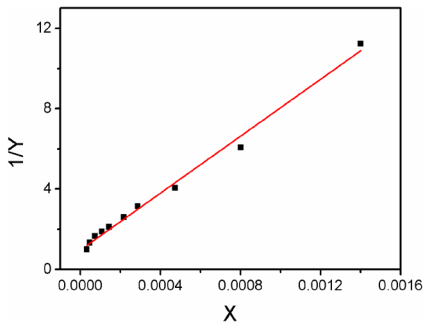

Figure 2. Plot of $1/Y$ versus X to give the intrinsic binding constants and binding number of SelP-H for Cu^+.

Supporting Information, Table S1). Using the known value for the formation constant of $Cu(BCA)_2$ of log β_2 = 17.3, the binding constant of log $K_{SelP\text{-}H}$ = 13.44 was calculated for Cu^+ binding to SelP-H.

The capacity of Aβ_{42} to compete for Cu^+ with BCA was compared. Previously, Cu^+ was suggested to be ligated by the His13 and His14 in a linear coordination environment in Aβ.[18] As shown in Figure 1B and Supporting Information, Figure S1, Aβ_{42} was unable to remove Cu^+ from the $Cu^+(BCA)_2$ complex in the presence of excessive peptides. Therefore, SelP-H binds Cu^+ more tightly than Aβ_{42}. In the case of Aβ_{42}, the side chain of glutamic acid-11 (Glu11) adjacent to His13 has a much

dx.doi.org/10.1021/ic4028282 | Inorg. Chem. 2014, 53, 1672–1678

lower pK_a value than that of His13, making it to be deprotonated preferentially. The negatively charged Glu11 may therefore stabilize the positively charged form of His and inhibit the deprotonation of His, therefore decreasing its affinity for Cu^+.

SelP-H Binds Cu^{2+} with High Affinity. Isotherm titration calorimetry (ITC) was used to characterize the thermodynamics of SelP-H binding with Cu^{2+}. Representative ITC data for the titration of Cu^{2+} into SelP-H in ACES buffer are shown in Figure 3. The isotherm was best fitted with the single binding sites model with n = 2.2 ± 0.1, and the buffer-dependent parameters were listed in Table 1.

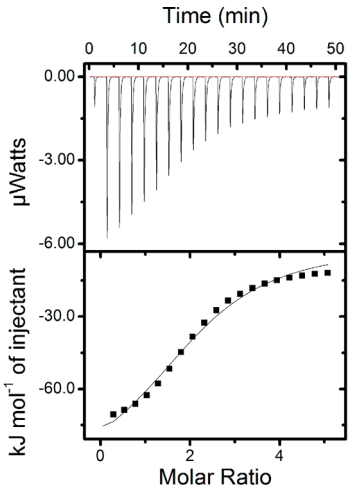

Figure 3. Calorimetric titration of Cu^{2+} (2 mM) to SelP-H (50 μM) in 20 mM ACES buffer, pH 7.4. (top) Raw data. (bottom) Plots of integrated heat versus the metal ion/protein ratio. The solid line represents the best fit for single binding site model. All experiments were carried out at 25 °C.

The binding of Cu^{2+} to SelP-H is an enthalpy (ΔH = −97.9 ± 5.7) but not entropy (ΔS = −234) driven reaction. ACES was chosen not only for its buffering capacity at the desired pH, but also for the formation of the well-defined $Cu^{2+}(ACES)_2$ complex. A recently reported method was used to extract buffer-independent binding constants.[19] The buffer-independent average dissociation constants of Cu^{2+} bound to SelP-H was calculated to be 0.9 nM (details in Supporting Information), which is much lower than the previously reported value for its binding to Aβ_{42} (50−90 nM).[20] The much higher binding affinity of copper in both oxidation states of Cu^+ and Cu^{2+} toward SelP-H compared with Aβ_{42} indicates that SelP-H might modulate the Cu^+/Cu^{2+}-induced aggregation and neurotoxicity of Aβ_{42}.

SelP-H Attenuates Cu^{2+}/ Cu^+-Induced Aβ_{42} Aggregation. The aggregation morphology and the extent of Aβ_{42} aggregation were investigated by TEM. To maximize the aggregate-free character of the amyloidogenic peptide at the zero time point, Aβ_{42} was treated with hexafluoroisopropanol (HFIP), which denatured the amyloid aggregates and dissociated the cross β-sheet structures. As shown in Figure 4A, Aβ_{42} aggregated intensively to form abundant ribbons and twisted chains of a complex of protofibrils and fibrils, after it

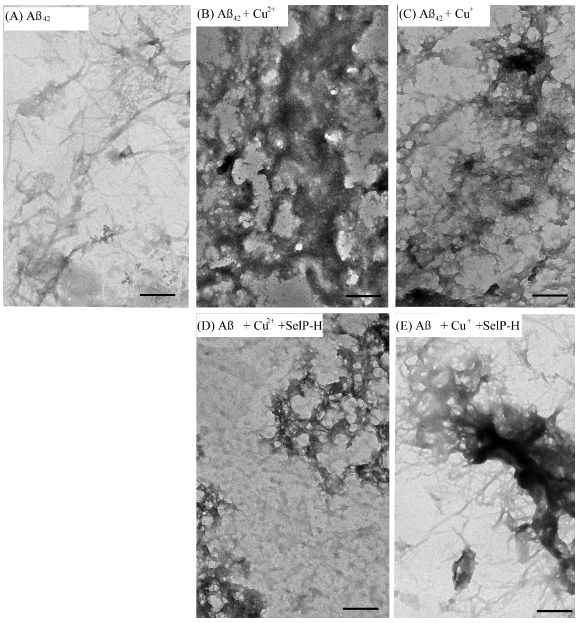

Figure 4. Transmission electron microscopy images of Aβ_{42} after incubation at 37 °C for 24 h. (A) Aβ_{42}. (B) Aβ_{42} with 1 mol equiv of Cu^{2+}. (C) Aβ_{42} with 1 mol equiv of Cu^{2+}. (D) Aβ_{42} with 1 mol equiv of Cu^{2+} as well as SelP-H. (E) Aβ_{42} with 1 mol equiv of Cu^+ as well as SelP-H. The final concentrations of SelP-H, Aβ_{42}, Cu^+, and Cu^{2+} are 10 μM. Cu^+ was prepared by reducing $CuSO_4$ with 1 mM ascorbate. Scale bar = 200 nm.

was incubated at 37 °C for 24 h. Previously, Cu^{2+} was observed to inhibit the fibrillization of Aβ_{42} and induce formation of nonfibrillar Aβ_{42} aggregates. Consistently, Aβ_{42} was grown into amorphous aggregates with much more aggregation when coincubated with 1 mol equiv of Cu^{2+} (Figure 4B). SelP-H inhibited Cu^{2+}-mediated Aβ_{42} aggregation and induced the formation of some amount of fibrils (Figure 4D). Cu^+ was reported to bind to Aβ_{42}; however, its effect on the aggregation and neurotoxicity of Aβ_{42} is still unclear. In our Study, we found Cu^+ exerted a similar effect on the aggregation of Aβ_{42} as Cu^{2+} but to a lower extent (Figure 4C). Similarly, SelP-H suppressed the nonfibrillar aggregation of Aβ_{42} caused by Cu^+ and rendered a large amount of Aβ_{42} growth to protofibrils and fibrils (Figure 4E).

The aggregation degrees of Aβ_{42} incubated with different additives (copper ions and SelP-H) were examined by ThT fluorescence assay. ThT specifically binds to the β-sheet of amyloid beta rapidly but not to monomers nor oligomers. Therefore the fluorescence intensity at 482 nm could be used to quantify Aβ fibrils. As shown in Figure 5, both Cu^+ and Cu^{2+} decreased the fluorescence intensity at 482 nm, in good agreement with the observation in TEM that copper ions inhibited the fibrillization of Aβ_{42}. The inhibitory effect of Cu^{2+} is slightly higher than that of Cu^+. SelP-H suppressed the effects

Table 1. Best-Fit Thermodynamic Parameters of Cu^{2+} Binding to SelP-H Obtained from ITC Measurements

N_{ITC}	K_{ITC} (×10^4)	ΔH_{ITC} [kcal mol^{-1}]	ΔS_{ITC} [cal mol^{-1} K]	K (×10^9)	K_D nM
2.2 ± 0.1	7.9 ± 1.2	−97.9 ± 5.7	−234	1.1 ± 0.2	0.9 ± 0.2

dx.doi.org/10.1021/ic4028282 | Inorg. Chem. 2014, 53, 1672−1678

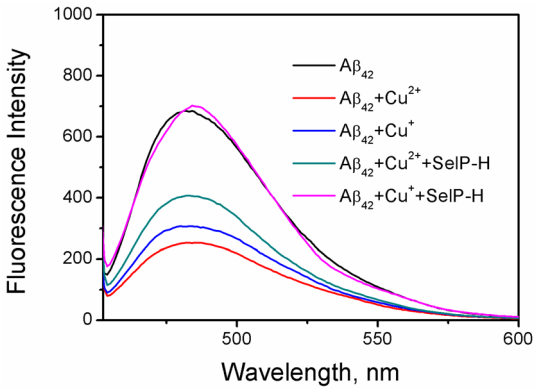

Figure 5. Effects of copper ions (10 μM) and SelP-H (10 μM) on fibrillation of Aβ_{42} (10 μM). All experiments were carried out in 50 mM Tris-HCl, 100 mM NaCl, containing 20 μM ThT at pH 7.4, 37 °C.

of copper ions and initiated the formation of fibrils, especially in the case of Cu^+. The result was in line with the TEM imaging.

SelP-H Attenuates Cu^{2+}/ Cu^+-Induced Aβ_{42} Neurotoxicity. Cell viability experiments with N2A cells were performed by CCK-8 assay to examine the protective effects of SelP-H against Aβ_{42} and metal ions. In our Study, Aβ_{42} was incubated at 37 °C for 24 h in the presence or absence of copper ions and/or SelP-H; that is, Aβ_{42} was grown to fibrils or metal-induced nonfibrillar aggregates before it was added to the cells. As shown in Figure 6A, lane 3, Aβ_{42} fibrils revealed a limited neurotoxicity (94.0 ± 1.8% cell viability) to N2A cells, supporting the previous report on low toxicity of Aβ_{42} fibrils.[21] Metal-associated Aβ species were suggested to be neurotoxic.[22] In our Work, we tested the neurotoxicity of Cu^{2+}- and Cu^+-induced Aβ_{42} aggregates, which shows 68.6 ± 0.2% and 76.2 ± 4.8% cell survival rates, respectively, upon the treatments (Figure 6A, lanes 4 and 6). Therefore, both Cu^{2+} and Cu^+ enhanced the toxicity of Aβ_{42} toward N2A cells. To validate the role of SelP-H, SelP-H was added to Cu^{2+}-Aβ_{42} or Cu^+-Aβ_{42} mixture preincubated at 37 °C for 1 h and coincubated for additional 24 h before it was added to cell culture media. As expected, SelP-H alleviated the neuronal cytotoxicity of both Cu^{2+}-Aβ_{42} and Cu^+-Aβ_{42} species (Figure 6A, lanes 5 and 7), suggesting that SelP-H removed Cu^{2+} and Cu^+ from their Aβ_{42} complexes and the free Aβ_{42} grown to fibrils, which are much less toxic than the Cu^{2+}-/Cu^+-induced Aβ_{42} aggregates.

SelP-H Surpresses ROS Production Induced by Cu^{2+}/ Cu^+-Aβ_{42} Aggregates. Metal ions including Zn, Cu, and Fe ions have been shown to promote Aβ aggregation, leading to the formation of reactive oxygen species (ROS) and inducing oxidative stress.[23] In our Work, the ROS levels in N2A cells upon treatment with Aβ_{42} fibrils or Cu^{2+}-/Cu^+-Aβ_{42} nonfibrillar aggregates in the presence or absence of SelP-H were detected with the fluorescent probe 2′,7′-dichlorodihydrofluorescein (DCFH) and quantified with flow cytometry. As shown in Figure 6B, lane 2, treatment with Aβ_{42} fibrils for 24 h promoted the ROS production in N2A cells by 1.34 ± 0.03-fold. The ability of Aβ_{42} to induce the production of ROS in cells has been addressed by several reports previously.[24] Interestingly, copper in both oxidation states of Cu^+ and Cu^{2+} dramatically promoted the generation of ROS, with 2.04 ± 0.17 and 1.69 ± 0.01-fold increases relative to the control (PBS treated cells), Figure 6B, lanes 3 and 5. Different from the case in Aβ_{42}-mediated ROS production and oxidative damage, which was

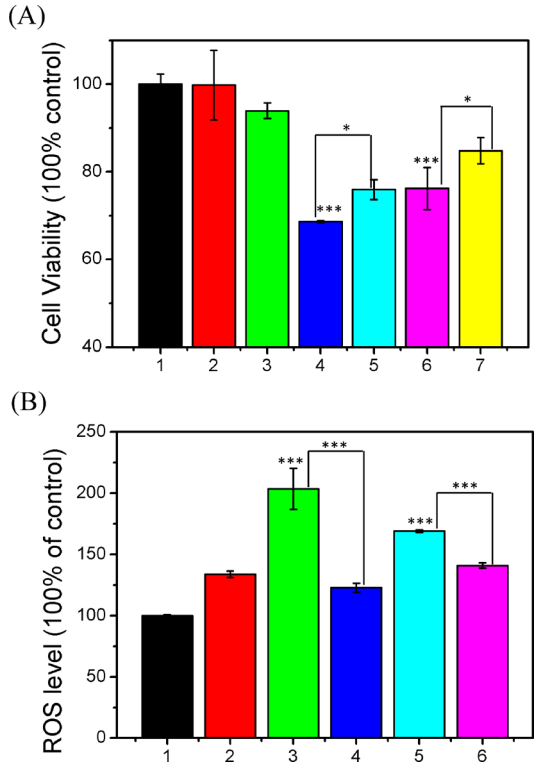

Figure 6. (A) CCK-8 cell viability assay of N2A cells upon treatment with: lane 1, the control experiment with PBS; lane 2, DMSO; lane 3, Aβ_{42} fibrils; lane 4, Cu^{2+}-Aβ_{42} nonfibrillar aggregates; lane 5, Cu^{2+}-Aβ_{42} nonfibrillar aggregates and SelP-H; lane 6, Cu^+-Aβ_{42} nonfibrillar aggregates; lane 7, Cu^+-Aβ_{42} nonfibrillar aggregates and SelP-H. (B) ROS level in N2A cells upon treatment with different Aβ_{42} aggregates. Lane 1, the control experiment with PBS; lane 2, Aβ_{42} fibrils; lane 3, Cu^{2+}-Aβ_{42} nonfibrillar aggregates; lane 4, Cu^{2+}-Aβ_{42} nonfibrillar aggregates and SelP-H; lane 5, Cu^+-Aβ_{42} nonfibrillar aggregates; and lane, 6 Cu^+-Aβ_{42} nonfibrillar aggregates and SelP-H. ROS in living N2A cells were monitored by a fluorescence assay kit consisting of 2′,7′-dichlorofluorescin diacetate and quantified with flow cytometry. The final concentrations of SelP-H, Aβ_{42}, and Cu^{2+}/Cu^+ are 10 μM. Cu^+ was prepared by reducing $CuSO_4$ with 1 mM H_2Asc. The results were obtained from the average of three experiments. *, $p < 0.05$; ***, $p < 0.001$.

mainly through the activation of the superoxide-producing enzyme nicotinamide adenine dinucleotide phosphate-oxidase,[24a,b,25] Cu^{2+}-/Cu^+-Aβ_{42} aggregates induced ROS generation mainly via the redox cycling of copper ions by the Fenton-type and Haber−Weiss-type reactions. As expected, SelP-H surpressed the ROS production mediated by Cu^{2+}-/Cu^+-Aβ_{42} aggregates by 77.9% and 40.7%, respectively (Figure 6B, lanes 4 and 6).

Cerebral spinal fluid contains micromolar levels of human serum albumin (HSA) but nanomolar levels of Aβ.[26] HSA binds Cu^{2+} with pM affinity using its amino terminal Cu(II)- and Ni(II) (ATCUN)-binding motif,[27] which is much stronger than the affinity reported between Cu^{2+} and monomeric Aβ (50−90 nM).[20] Consequently, the likelihood of in vivo formation of Cu^{2+}-Aβ complex is a contentious issue. Note that Aβ fibrils bind Cu^{2+} in the picomolar range,[28] which means fibrils are capable of competing for Cu^{2+} even in the presence of HSA. Unlike in plasma where extracellular copper is presumed to be Cu^{2+}, the concentration of ascorbate present in extracellular spinal fluid is sufficient to generate Cu^+.[29] The strong square-planar geometry of the ATCUN motif of HSA

dx.doi.org/10.1021/ic4028282 | Inorg. Chem. 2014, 53, 1672−1678

does not support the lower coordination number and tetrahedral coordination geometry favored by Cu^{+}; therefore, the monomeric Aβ preferentially binds Cu^{+} rather than Cu^{2+} in vivo.[30] It is very likely that in vivo Cu^{+} rather than Cu^{2+} induced the aggregation of Aβ from a soluble monomer to an insoluble aggregate. In our Work, we found that Cu^{+} rendered Aβ_{42} less aggregated and therefore induced lower intracellular ROS level and presented less neurotoxicity than Cu^{2+}. Shearer and Szalai demonstrated that the Cu^{+}-Aβ complex is sluggish to react with O_2, which decreases turnover to produce ROS.[7] Studies regarding Cu^{+} and Aβ in different aggregation states, especially soluble oligomer, which is the well-established most neurotoxic species, are worthy to carry out.

Among the 25 human selenoproteins, SelP is widely expressed in the brain and is involved in the onset and progression of AD; however, the underlying mechanisms of this are far from clear. In SelP, there are three domains (N-terminal region, C-terminal region, and His-rich domain, SelP-H) predicated on the surface of the protein. The functions of the N-terminus and C-terminus were previously reported to encompass oxidant defense and Se homeostasis.[10] However, the His-rich domain was less studied. In previous work, we found SelP-H bound transition metal ions and surpressed Zn^{2+}-mediated Aβ_{42} aggregation, ROS generation, and toxicity. Here we extended the roles of SelP-H to regulate both Cu^{+} and Cu^{2+}-mediated aggregation and neurotoxicity of Aβ_{42}.

CONCLUSIONS

The thermodynamic properties of SelP-H binding Cu ions in both oxidation states of Cu^{+} and Cu^{2+} were explored by spectroscopic and calorimetric methods. SelP was demonstrated to coordinate 2 and 1 mol equiv of Cu^{2+} and Cu^{+} with dissociation constants of 0.9 nM and 3.7×10^{-14} M, respectively. Copper ions binding to Aβ_{42} almost completely surpressed Aβ_{42} fibrillization and induced the formation of amorphous aggregates, which are more neurotoxic than the fibrils. Compared to Cu^{2+}, Cu^{+} presented a much milder effect. SelP-H significantly inhibited the nonfibrillar aggregation of Aβ_{42} induced by Cu^{2+} and Cu^{+}, and it initiated the formation of some amount of fibrils. Interestingly, SelP-H attenuated Cu^{2+}/Cu^{+}-Aβ_{42}-induced neurotoxicity and the intracellular ROS production in living cells. It was reported that SelP is colocalized with Aβ plaques in the post-mortem tissues from individuals with the hallmark lesions of AD.[12] These studies suggest that in addition to its roles in Se homeostasis and oxidant defense, SelP may play certain roles in regulating redox balance as well as in metal homeostasis. In vivo studies using AD model mouse are underway to better understand the role of SelP in the brain and AD progress.

ASSOCIATED CONTENT

Supporting Information

Figure S1on the competition for Cu^{+} between Aβ_{42} and BCA and Table S1 on the determination of intrinsic binding constants and binding number of SelP-H for Cu^{+} by competition with BCA for Cu^{+}. Supplementary methods on "One set of sites binding model" and "Estimation of buffer-independent Cu^{2+} binding constants". This material is available free of charge via the Internet at http://pubs.acs.org.

AUTHOR INFORMATION

Corresponding Author

*E-mail: liuqiong@szu.edu.cn. Phone: 86-755-26534152.

Author Contributions

§These authors contributed equally.

Notes

The authors declare no competing financial interest.

ACKNOWLEDGMENTS

This work was financially supported by the National Natural Science Foundation of China (No. 31070731, 21271131, 21301120, 81372984) and the Shenzhen Bureau of Science, Technology and Information (No. JCYJ20120817163755064). The TEM used in this work was supported by the Institute for Advanced Materials (IAM) with funding from the special Equipment Grant from the University Grants Committee of the Hong Kong Special Administrative Region, China (SEG_HKBU06).

REFERENCES

(1) Goedert, M.; Spillantini, M. G. *Science* **2006**, *314* (5800), 777–781.
(2) Selkoe, D. J.; Podlisny, M. B. *Annu. Rev. Genomics Hum. Genet.* **2002**, *3*, 67–99.
(3) (a) Roher, A. E.; Lowenson, J. D.; Clarke, S.; Woods, A. S.; Cotter, R. J.; Gowing, E.; Ball, M. J. *Proc. Natl. Acad. Sci. U.S.A.* **1993**, *90*, 10836–10840. (b) Jarrett, J. T.; Berger, E. P.; Lansbury, P. T., Jr. *Biochemistry* **1993**, *32*, 4693–4697.
(4) (a) McGowan, E.; Pickford, F.; Kim, J.; Onstead, L.; Eriksen, J.; Yu, C.; Skipper, L.; Murphy, M. P.; Beard, J.; Das, P.; Jansen, K.; Delucia, M.; Lin, W. L.; Dolios, G.; Wang, R.; Eckman, C. B.; Dickson, D. W.; Hutton, M.; Hardy, J.; Golde, T. *Neuron* **2005**, *47*, 191–199. (b) Kuperstein, I.; Broersen, K.; Benilova, I.; Rozenski, J.; Jonckheere, W.; Debulpaep, M.; Vandersteen, A.; Segers-Nolten, I.; Van Der Werf, K.; Subramaniam, V.; Braeken, D.; Callewaert, G.; Bartic, C.; D'Hooge, R.; Martins, I. C.; Rousseau, F.; Schymkowitz, J.; De Strooper, B. *EMBO J.* **2010**, *29*, 3408–3420. (c) Pauwels, K.; Williams, T. L.; Morris, K. L.; Jonckheere, W.; Vandersteen, A.; Kelly, G.; Schymkowitz, J.; Rousseau, F.; Pastore, A.; Serpell, L. C.; Broersen, K. *J. Biol. Chem.* **2012**, *287* (8), 5650–60.
(5) Gaggelli, E.; Kozlowski, H.; Valensin, D.; Valensin, G. *Chem. Rev.* **2006**, *106*, 1995–2044.
(6) Adlard, P. A.; Bush, A. I. *J. Alzheimer's Dis.* **2006**, *10*, 145–163.
(7) Shearer, J.; Szalai, V. A. *J. Am. Chem. Soc.* **2008**, *130*, 17826–17835.
(8) Arbiser, J. L.; Kraeft, S. K.; van Leeuwen, R.; Hurwitz, S. J.; Selig, M.; Dickersin, G. R.; Flint, A.; Byers, H. R.; Chen, L. B. *Mol. Med.* **1998**, *4*, 665–670.
(9) Luo, Y.; Xu, Y.; Bao, Q.; Ding, Z.; Zhu, C.; Huang, Z. X.; Tan, X. *J. Biol. Inorg. Chem.* **2013**, *18* (1), 39–47.
(10) (a) Hoffmann, P. R.; Hoge, S. C.; Li, P. A.; Hoffmann, F. W.; Hashimoto, A. C.; Berry, M. J. *Nucleic Acids Res.* **2007**, *35*, 3963–3973. (b) Burk, R. F.; Hill, K. E. *Annu. Rev. Nutr.* **2005**, *25*, 215–235.
(11) Lu, T.; Pan, Y.; Kao, S. Y.; Li, C.; Kohane, I.; Chan, J.; Yankner, B. A. *Nature* **2004**, *429*, 883–891.
(12) Bellinger, F. P.; He, Q. P.; Bellinger, M. T.; Lin, Y.; Raman, A. V.; White, L. R.; Berry, M. J. *J. Alzheimer's Dis.* **2008**, *15*, 465–472.
(13) Takemoto, A. S.; Berry, M. J.; Bellinger, F. P. *Ethn. Dis.* **2010**, *20*, S1–92–95.
(14) Du, X.; Li, H.; Wang, Z.; Qiu, S.; Liu, Q.; Ni, J. *Metallomics* **2013**, *5*, 861–870.
(15) Xiao, Z.; Donnelly, P. S.; Zimmermann, M.; Wedd, A. G. *Inorg. Chem.* **2008**, *47*, 4338–4347.
(16) (a) Yatsunyk, L. A.; Rosenzweig, A. C. *J. Biol. Chem.* **2007**, *282*, 8622–8631. (b) Du, X.; Li, H.; Wang, X.; Liu, Q.; Ni, J.; Sun, H. *Chem. Commun.* **2013**, *49*, 9134–9136.
(17) Yatsunyk, L. A.; Rosenzweig, A. C. *J. Biol. Chem.* **2007**, *282*, 8622–8631.
(18) Shearer, J.; Szalai, V. A. *J. Am. Chem. Soc.* **2008**, *130*, 17826–17835.

(19) Jois, P. S.; Madhu, N.; Rao, D. N. *Biochem. J.* **2008**, *410*, 543−553.
(20) Tougu, V.; Karafin, A.; Palumaa, P. *J. Neurochem.* **2008**, *104*, 1249−1259.
(21) Sharma, A. K.; Pavlova, S. T.; Kim, J.; Finkelstein, D.; Hawco, N. J.; Rath, N. P.; Mirica, L. M. *J. Am. Chem. Soc.* **2012**, *134*, 6625−6636.
(22) Bush, A. I.; Tanzi, R. E. *Neurotherapeutics* **2008**, *5*, 421−432.
(23) (a) Faller, P.; Hureau, C. *Dalton Trans.* **2009**, *7*, 1080−1094. (b) Molina-Holgado, F.; Hider, R. C.; Gaeta, A.; Williams, R.; Francis, P. *BioMetals* **2007**, *20*, 639−654.
(24) (a) Park, L.; Anrather, J.; Zhou, P.; Frys, K.; Pitstick, R.; Younkin, S.; Carlson, G. A.; Iadecola, C. *J. Neurosci.* **2005**, *25*, 1769−1777. (b) Park, L.; Zhou, P.; Pitstick, R.; Capone, C.; Anrather, J.; Norris, E. H.; Younkin, L.; Younkin, S.; Carlson, G.; McEwen, B. S.; Iadecola, C. *Proc. Natl. Acad. Sci. U.S.A.* **2008**, *105*, 1347−1352. (c) Girouard, H.; Iadecola, C. *J. Appl. Physiol.* **2006**, *100*, 328−335.
(25) (a) Chaney, M. O.; Stine, W. B.; Kokjohn, T. A.; Kuo, Y. M.; Esh, C.; Rahman, A.; Luehrs, D. C.; Schmidt, A. M.; Stern, D.; Yan, S. D.; Roher, A. E. *Biochim. Biophys. Acta* **2005**, *1741*, 199−205. (b) Zhu, D.; Hu, C.; Sheng, W.; Tan, K. S.; Haidekker, M. A.; Sun, A. Y.; Sun, G. Y.; Lee, J. C. *Biochem. J.* **2009**, *421*, 201−210.
(26) Mayeux, R.; Tang, M. X.; Jacobs, D. M.; Manly, J.; Bell, K.; Merchant, C.; Small, S. A.; Stern, Y.; Wisniewski, H. M.; Mehta, P. D. *Ann. Neurol.* **1999**, *46*, 412−416.
(27) Rozga, M.; Sokolowska, M.; Protas, A. M.; Bal, W. *J. Biol. Inorg. Chem.* **2007**, *12*, 913−918.
(28) Sarell, C. J.; Syme, C. D.; Rigby, S. E.; Viles, J. H. *Biochemistry* **2009**, *48*, 4388−4402.
(29) Rice, M. E. *Trends Neurosci.* **2000**, *23*, 209−216.
(30) Feaga, H. A.; Maduka, R. C.; Foster, M. N.; Szalai, V. A. *Inorg. Chem.* **2011**, *50*, 1614−1618.